Flow chamber analysis of size effects in the adhesion of spherical particles

P Decuzzi[1,3]
F Gentile[1]
A Granaldi[3]
A Curcio[2]
F Causa[1]
C Indolfi[2]
P Netti[4]
M Ferrari[5]

[1]Center of Bio-/Nanotechnology and -/Engineering for Medicine and [2]Division of Cardiology, University of Magna Graecia at Catanzaro, Viale Europa – Loc. Germaneto, Catanzaro, Italy; [3]Center of Excellence in Computational Mechanics, Politecnico di Bari, Bari, Italy; [4]Interdisciplinary Research Centre in Biomaterials, University of Naples – Federico II, Naples, Italy; [5]The University of Texas Health Science Center, and M.D. Anderson Cancer Center and Rice University, Houston, Texas, USA

Abstract: The non-specific adhesion of spherical micro- and nano-particles to a cell substrate is investigated in a parallel plate flow chamber. Differently from prior in-vitro analyses, the total volume of the particles injected into the flow chamber is kept fixed whilst the particle diameter is changed in the range 0.5–10 μm. It is shown that: (i) the absolute number of particles adherent to the cell layer per unit surface decreases with the size of the particle as $d^{-1.7}$; (ii) the volume of the particles adherent per unit surface increases with the size of the particles as $d^{+1.3}$. From these results and considering solely non-specific particles, the following hypothesis are generated (i) use the smallest possible particles in biomedical imaging and (ii) use the largest possible particles in drug delivery.

Keywords: bio-adhesion, particulates, flow chamber, in-vitro experiments

Introduction

Advances in nanosciences and micro/nanofabrication techniques have led to novel strategies and devices for drug delivery and diagnosis in biomedical applications (La Van et al 2003). In particular, biomimetic artificial carriers are emerging as powerful tools for cancer and heart diseases (Ferrari 2005). These are particulates carrying therapeutic or imaging agents administered at the systemic level and delivered towards a specific biological target, for instance a tumoral cell or the tumor microenvironment.

The surface of these particulates can be coated by ligand molecules that can recognize countermolecules (receptors) expressed over the biological target by means of specific interactions (ligand-receptor interactions). On the other hand, if ligand molecules are not distributed over the particle surface, the target recognition is mediated by non-specific interactions such as van der Waals, electrostatic and steric forces (Decuzzi et al 2005).

The power of intravascularly injectable particles over freely administered molecules lies in their multifunctionality and engineerability. In fact, the use of particles delivery affords substantial advantages including (i) the specific biomolecular targeting through one or more conjugated antibodies or other recognition molecules; (ii) ability to carry one or more therapeutic agents; (iii) signal amplification for imaging through co-encapsulated contrast agents; (iv) tuning of the physico-chemical and geometrical properties that favors avoidance of the biological and physiological barriers and improve the recognition of the target cells or microenvironments.

A broad spectrum of particulates have been presented in the literature which can be used both in medical therapy and imaging. These have different sizes, ranging from few tens of nanometers (dendrimers) (Choi et al 2005), to hundreds of nanometers (polymer particles and liposome) (Crommelin and Schreier 1994; Duncan 2003), up to few microns (silicon and silica based particles) (Cohen et al 2003); different shapes, from the classical spheres, to spheroids (van Dillen et al 2004) and even more complex

Correspondence: Paolo Decuzzi
Email p.decuzzi@poliba.it

shapes (Rolland et al 2005) and with different composition and chemico-physical properties. Since these particulates can be engineered by changing size, shape and surface chemico-physical properties, it is of great importance to investigate if any combination exists of these design parameters leading to the optimal particle. This is the particle with the largest recognition efficacy and selectivity which has the ability to bind firmly to the biological target and direct the therapeutic or imaging agent to the right site at the right time.

In 2001, Goetz and colleagues have analyzed the effect of the size of micrometric spherical particles on their adhesion performance to a P-selectin substrate under in-vitro flow conditions. Since they were interested in studying the specific interaction of circulating leukocytes with endothelial cells, they employed 5, 10, 15, and 20 μm diameter microspheres coated with a specific ligand targeted against a P-selectin substrate. They showed that the adhesive strength of the particles, expressed in terms of the critical shear stress and rolling velocity, is significantly influenced by the diameter of the particles, and as the particle size increases the critical shear stress reduces making firm adhesion less likely. Despite this work, at authors' knowledge, no other experimental study has been devoted to the analysis of size effects in micro- and nano-particles adhesion. In this work, the focus is on spherical particles not coated with ligand molecules and with a size ranging from 0.5 μm up to 0.10 μm. The adhesive performances of these particles is assessed in terms of the number of particles adhering non-specifically to a confluent layer of endothelial cells under fixed hydrodynamic conditions in a parallel plate flow chamber.

Materials and methods

Parallel plate flow chamber

A Glycotech (Rockville, MD, USA) parallel plate flow chamber was used as described by Brown and Larson (2001) . It consists of a Plexiglas flow deck with an inlet and an outlet hole, a silicon gasket and a circular 35 mm tissue culture borosilicate dish. The flow chamber was connected to a Harvard Apparatus syringe pump through the inlet hole and to a reservoir through the outlet hole. The channel within the flow chamber was defined by a silicon rubber gasket sitting between the flow deck and the microscope 35 mm dish. The gasket used in the present experiments had a thickness h of 0.01 in and a width w of 1 cm. The volumetric flow rate Q defined through the syringe pump was fixed to be equal to 50 μl/min for all the experiments. Based on these data, the mean velocità U (= $Q/(wh)$) within the chamber was of about 0.328 mm/sec, a physiologically relevant value for human capillaries (Ganong 2003). The shear rate S at the substrate was given by the commonly used relation

$$S = 6Q/(h^2 w) = 7.75\text{sec}^{-1} \quad (1)$$

and the shear stress at the wall $(\mu S)_w = 7.75 \times 10^{-3}$ *Pa* being $\mu = 10^{-3}$ *Pa* × sec the viscosity of water. The shear rate and the shear stress were sufficiently small to allow for the non-specific adhesion of particles to cells. Experiments were carried out at room temperature (24 °C).

Measuring microsphere attachment

After assembling the flow chamber on the stage of an inverted microscope, a region at the center of the channel was chosen with a sufficiently large number of confluent cells (region of interest). In this central region the flow was not disturbed by the inlet and outlet ports and by the lateral chamber walls so that a fully developed linear laminar flow could be considered in proximity of the chamber floor. The microscope objective with a 10x lens was focused on this region and after a short rinse, the flow with the particles entered the chamber.

Using the fluorescent module of the microscope, the flow of the particles in the region of interest was recorded during the whole experiments. Each experiment lasted between 800 and 1000 sec. The size of the region of interest was of 750×750 μm^2 and it was mapped into 256×256 lines. With such a resolution and a line frequency of 800 Hz, the acquisition rate was of about *3 fps* (800/256 = 3.125 *fps*). Such a scan speed was fast enough to follow the motion of the particles with no jumps or discontinuities. Each acquired frame was then converted and exported to MatLab® (MatLab 6.5), where it was analyzed by means of standard image-analysis tools. The total number of particles adherent to the substrate n_{tot} within the region of interest, the number of particles adherent to the sole cells n_c within the region of interest and the number of particles adherent to the sole borosilicate dish n_d were measured as a function of the frame number, which was easily converted in time by knowing the acquisition rate.

Cell culture

Human umbilical vein endothelial cells (HUVECs) were purchased from Cambrex, Inc. (East Rutherford, NJ, USA). Cells were maintained in EGM-2 – Endothelial Cell Medium-2 (Cambrex Bio Science Walkersville Inc., MD) supplemented with 2% FBS, 0.04% hydrocortisone, 0.4% hFGF-B, 0.1% VEGF, 0.1% rIGF-1, 0.1% ascorbic acid, 0.1% hEGF, 0.1% GA-1000, 0.1% heparin, 100 U/mL penicillin, and 100 μg/mL streptomycin and were grown at

37 °C with humidified 95% air/5% CO_2. HUVEC were used for experiments at passages 3 to 4.

For each experiment, cells were plated on a borosilicate dish with a 0.2 mg/cm^2 substratum of type A gelatine (Sigma-Aldrich Corporation, MO, USA). When HUVECs reached 80% confluence, with an average cell-to-plate area of 35%, the borosilicate dish was detached from the bottom of the plate and mounted in the parallel plate flow chamber for particle-cell adhesion analysis. An image of the fluorescent particles adherent to the culture dish and to the cells is shown in Figure 1 for the 1 μm particle.

Particles

Fluoresbrite® Microspheres from Polysciences were used. These are Yellow Green fluorescent particles with an excitation maximum at 441 nm and an emission maximum at 486 nm. Particles with different sizes were purchased, namely 10, 6, 1, 0.75 and 0.50 μm. The number of injected particles changes with their size so that the total volume of injected particle is kept equal to $V_{tot} \approx 5.2 \times 10^7$ μm^3. The concentration of the particles for each size is listed in Table 1. The relative density of the spheres with respect to the water is of 50 kg/m^3. A 1 ml syringe is used to perfuse the particles, dispersed in a physiological solution, within the flow chamber.

Results

The number of adherent particles within the region of interest has been measured for the five different sizes analyzed (0.50, 0.75, 1, 6 and 10 μm) as a function of time and for the whole duration of the experiment. For each particle size, at least 10 different experiments have been carried out, and the experiments considered as statistically significant were 4 for the 10, 6, and 0.75 μm particles; 8 for the 1 μm particle and 3 for the 0.5 μm particle. As the experiment progress in time, the number of adherent particles grows. For the smaller particles (0.50 and 0.75 μm), it is observed that the number of adherent particles increases almost linearly initially, that it to say an almost constant adhesion rate (number of particles per time). As the end of the experiment is approached, the adhesion rate reduces and tends to zero which seems to correspond to a saturation of the substrate by the particles adhering within the region of interest. For the larger particles, the adhesion rate is always positive and no saturation can be observed within the characteristic experiment duration. In Figures 2 and 3, the experimental data related to the 0.5 and 1 μm particles are shown: the lower curve is for the n_c particles adhering to the cells solely and the upper curve for the total number n_{tot} of particles adhering within the whole region of interest. The difference between n_{tot} and n_c gives simply the number of particles n_d adherent over the sole borosilicate dish.

By fixing the size of the particles and averaging over a significant number of experiments, the variation of the mean number of adherent particles and the corresponding standard deviation can be plotted as a function of time for each particle size. In Figure 4, the absolute number n_{tot}, n_c and n_d of particles measured at the end of the experiments (about 800 sec) is plotted as a function of the particle diameter a. In a double logarithm diagram, the experimental data are distributed along three straight lines: the line with black boxes is for the n_c particles adhering over the cells; the line with the white pentagons is for the n_d particles adhering over the borosilicate dish and the line with white triangles is for the n_{tot} particles adhering within the whole region of interest. As the diameter a of the particle reduces, the number of adherent particles n_{tot}, n_d and n_c increases, as it results from the relations

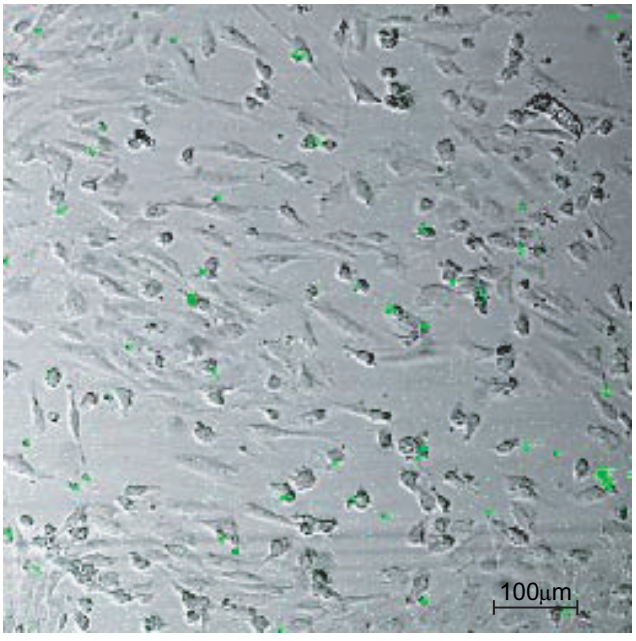

Figure 1 An image showing 1 μm particles adherent to the cells and to the borosilicate dish (substrate) in the region of interest.

Table 1 Particles concentration versus particles size for a fixed total particle volume $V = 5.2 \times 10^7$ μm^3

d [μm]	χ [*particles/ml*]
0.5	8×10^8
0.75	2.37×10^8
1.0	10^8
6.0	4.63×10^5
10.0	10^5

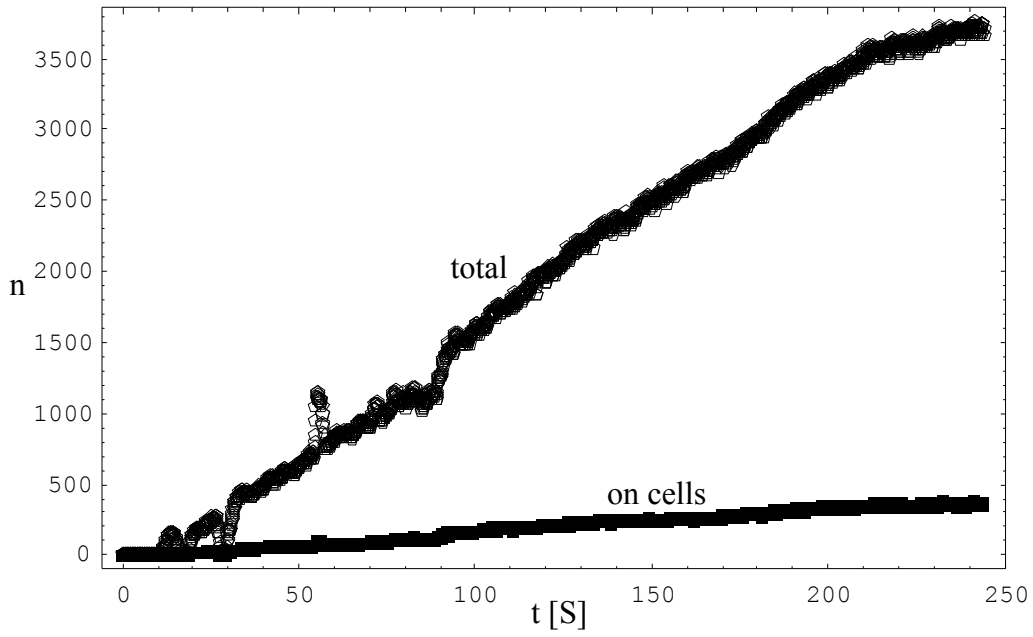

Figure 2 The variation of the number *n* of adherent particles with time (d = 0.50 μm). The upper curve is for the total number of adherent particles n_{tot}, whereas the lower curve is for the particles adherent solely to the cells n_c.

$$n_{tot} = 627.96\ d^{-1.696};\ n_d = 377\ d^{-2.15};\ n_c = 164.754\ d^{-1.143} \quad (2)$$

derived by a non linear regression of the experimental data, with *a* expressed in μm. The total number of particles n_{tot} is evidently larger than n_c and n_d, by definition.

Differently, in Figure 5, the number of adherent particles per unit surface, ie, the particle surface density, is shown as a function of the diameter *a*. The total number of adherent particles n_{tot} is normalized by the area of the region of interest, the number of particles adherent to the sole cells n_c is normalized by the area occupied by the cells within the region of interest, and the number of particles n_d adhering over the sole borosilicate dish is normalized over the area of the whole region of interest free of cells. In a double logarithm diagram, the three cited surface densities ($\tilde{n}_{tot}$, $\tilde{n}_d$ and $\tilde{n}_c$) are well aligned along three straight and almost parallel lines (Figure 5). Again, the line with black boxes is for the $\tilde{n}_c$ particles adhering over the cells per unit cell surface; the line with the white triangles is for the $\tilde{n}_d$ particles adhering over the borosilicate dish per unit surface of free dish and the line with white pentagons is for the $\tilde{n}_{tot}$ particles adhering within the whole region of interest per unit surface. A non linear regression of the experimental data leads to the following relations

$$\tilde{n}_{tot} = 1116.39\ d^{-1.696};\ \tilde{n}_d = 783\ d^{-2.04};\ \tilde{n}_c = 2784.34\ d^{-1.746} \quad (3)$$

with *a* expressed in μm. From the above approximate relations and the data plotted in Figure 5, it derives that the particles prefer to adhere to the cells than to the borosilicate dish: for $d = 10$ μm, the average values for $\tilde{n}_c$ and $\tilde{n}_d$ are respectively 50 and 7 μm^{-2}, with $\tilde{n}_c \approx 7\ \tilde{n}_d$; whereas for $d = 0.5$ μm, the average values for $\tilde{n}_c$ and $\tilde{n}_d$ are respectively 9300 and 3220 μm^{-2}, with $\tilde{n}_c \approx 3\ \tilde{n}_d$.

Discussions

Particle sedimentation and non-specific interactions

The motion of the particles within the flow chamber is governed by different types of forces. These are hydrodynamic forces, gravitational forces, diffusional forces and non-specific forces exerted over the particle, as the van der Waals, electrostatic and steric interactions (Decuzzi et al 2005). Due to the width-to-height ratio of the flow chamber (1 cm to 254 μm), in the center of the chamber and in close proximity to the substrate, a linear laminar flow field can be assumed. Due to the linearity of the equations of flow, the longitudinal and vertical components of the particle motion are independent and can be treated separately. Therefore, particles dynamics can be described by the two following uncoupled equations

$$m\frac{d^2x}{dt^2} = F_x\ ; \quad m\frac{d^2z}{dt^2} = F_z \quad (4)$$

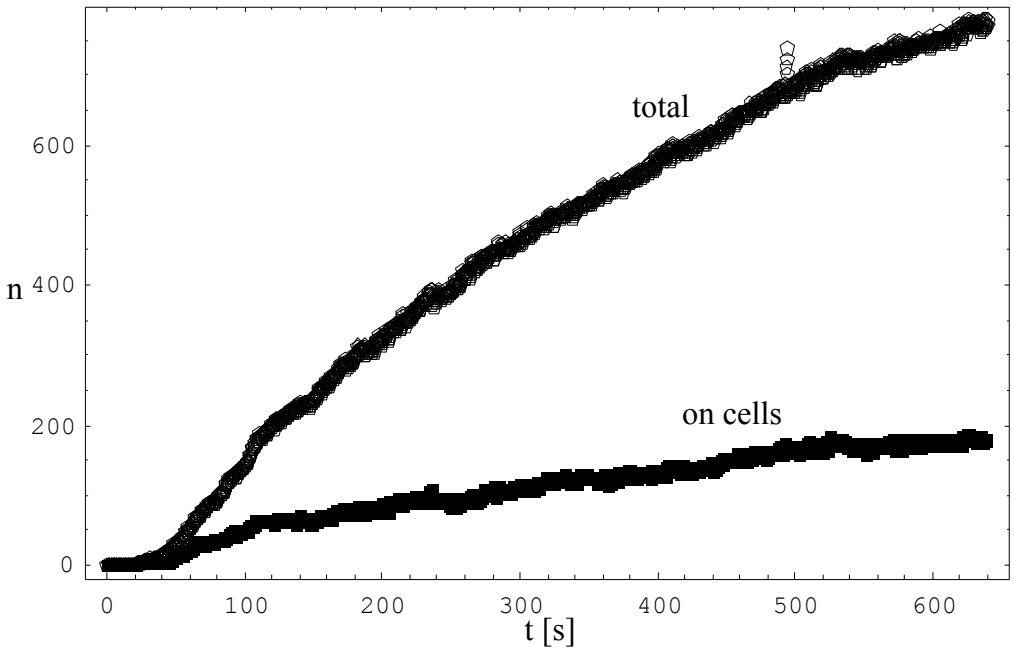

Figure 3 The variation of the number n of adherent particles with time (d = 1.0 μm). The upper curve is for the total number of adherent particles n_{tot}, whereas the lower curve is for the particles adherent solely to the cells n_c.

being F_x and F_z the resultants of the force applied over the particle in the longitudinal (x) and vertical (z) directions, respectively, and m the particle inertial mass. Notice that by invoking (4), the particles have been assumed as material points neglecting any interaction of the particles with the flow field, and any particle rotation. The approach (sedimentation) of the particles from the free stream to the substrate is governed solely by F_z; whereas the longitudinal drag force F_x is responsible for its motion along the channel from the inlet to the outlet port. Due to the large number of particles injected into the chamber (see Table 1), it is further assumed that the particles are distributed almost uniformly in the entrance cross section of the chamber.

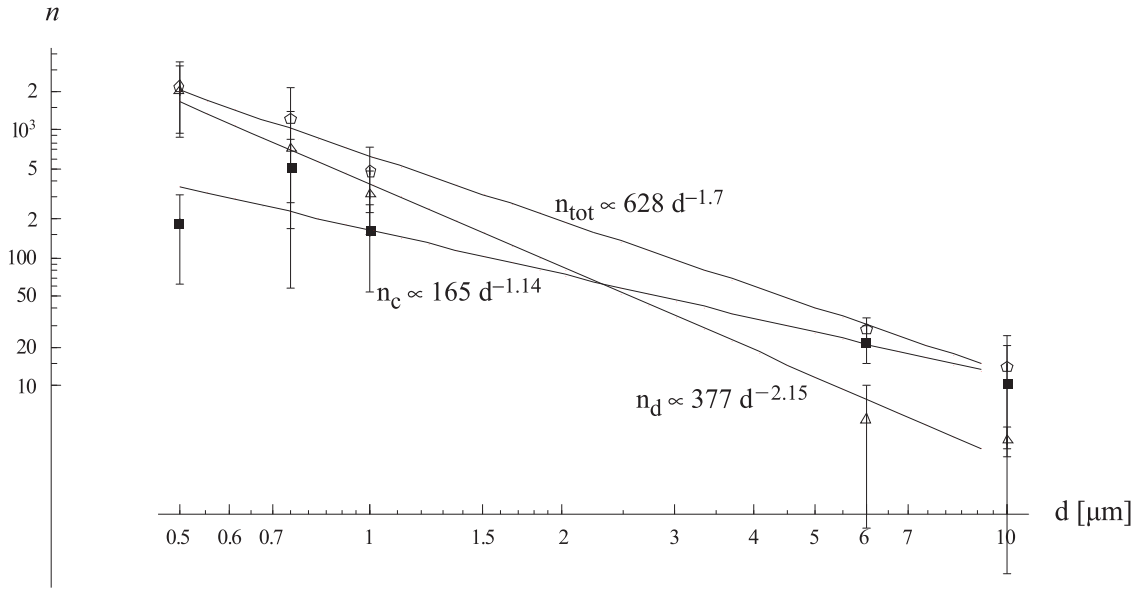

Figure 4 The variation of the total number of particles (n_{tot} white pentagons), of the number of particles adherent to the cells (n_c black boxes), of the number of particles adherent to the borosilicate dish (n_d white triangles) with the particle diameter a at the end of the experiment (800 sec).

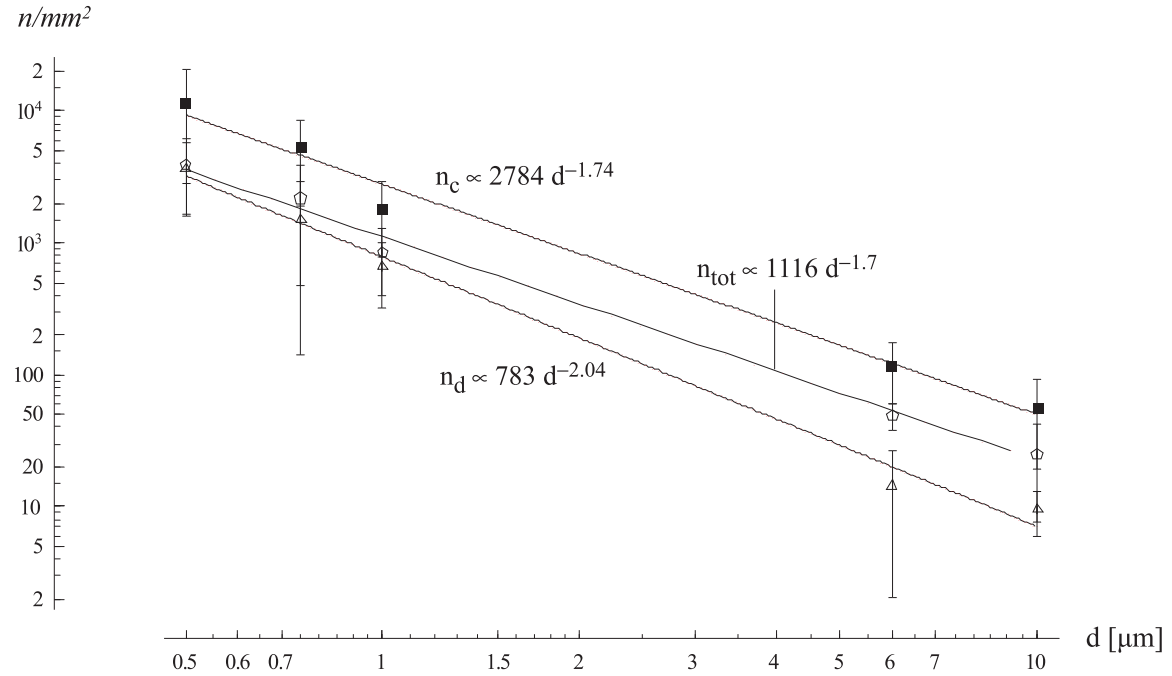

Figure 5 The variation of the surface density of the total number of particles ($\tilde{n}_{tot}$ white pentagons), of the number of particles adherent to the cells ($\tilde{n}_c$ black boxes), of the number of particles adherent to the borosilicate dish ($\tilde{n}_d$ white triangles) with the particle diameter *a* at the end of the experiment (800 sec).

Among all the particles injected into the flow chamber, only those that are sufficiently close to the substrate could have the chance to sediment and adhere to the substrate before leaving the chamber. Therefore, a 'boundary layer' with thickness *H* is identified within which are comprised solely those particles candidate to sediment onto the substrate. *H* is called as the 'sedimentation distance' and its dependence on *a* and *S* is derived in the sequel.

Notice that for an unbounded flow field, the sedimentation speed v_z of a particle with diameter *a* is directly given by the Stokes' law as

$$v_z = \frac{1}{18}\frac{\Delta\rho}{\mu}d^2 \propto d^2 \tag{5}$$

The time t_x needed for a particle to move over the total length L (= 2 cm) of the chamber is related to the longitudinal translational velocity v_x of the particle as

$$t_x = \frac{L}{v_x} \propto (Sd)^{-1} \tag{6}$$

where v_x has been shown to be proportional to *Sa* for particles sufficiently smaller than the chamber height (Goldman et al 1967). Therefore, the thickness of the boundary layer *H* has the form

$$H = v_z t_x \propto S^{-1} d\,. \tag{7}$$

Observing that in this work, rather than fixing the number of particles injected into the flow chamber, it has been fixed the total volume of the particles V_{tot}, it follows that the number of the particles *n* injected into the flow chamber increases as the size of the particles reduces and is proportional to d^{-3}, being

$$V_{tot} = n\frac{\pi}{6}d^3;\; n = \frac{6V_{tot}}{\pi}d^{-3} \tag{8}$$

Recalling the assumption of an uniform distribution of the particles within the entrance cross section of the chamber, the number of particles per unit surface within the sedimentation distance *H*, that is the particles candidate to adhere to the substrate, is given by

$$\tilde{n} = \frac{n}{V_{tot}}H \propto d^{-3}d = d^{-2} \tag{9}$$

The theoretical relation determined above between $\tilde{n}$ and a gives an exponent (–2) extraordinarily close to that derived experimentally for the density $\tilde{n}_d$ of the particles adherent onto the borosilicate dish (see the relation (3)). This theoretical exponent is also not far from that derived experimentally for the density of the particles adherent to the cells $\tilde{n}_c$, being *–1.75* just *15%* lower than 2. This slight difference between $\tilde{n}_c$ and $\tilde{n}_d$ could possibly be associated with the generation of adhesive non-specific interactions at the cell-particle interface larger than those arising at the particle-dish interface. These could be van der Waals and electrostatic forces favoring the sedimentation and subsequent firm adhesion of the larger particles over the elastic cell membrane compared to a rigid borosilicate dish (Decuzzi et al 2005). This hypothesis is also supported by the evidence that the difference between $\tilde{n}_c$ and $\tilde{n}_d$ reduces as a reduces, and by the fact that the absolute value of the non-specific forces reduces with the size of the particles.

Based on this, it can be derived that whilst for the particles adherent to the borosilicate dish the experimentally determined $\tilde{n}_d$ is mainly related to sedimentation, for the particles adherent to the cells the experimentally determined $\tilde{n}_c$ is related to sedimentation and to a small contribution of non-specific forces arising at the cell-particle interface.

Particle diffusion

As it regards the contribution of the Brownian diffusion to the particle adhesion, this can be approximately derived observing that the diffusive flux Φ of the particles across a reference plane parallel to the substrate is proportional to the diffusion coefficient D and to the concentration gradient across the surface. This particle flux Φ gives the number of particles per unit surface and unit time crossing the reference plane and heading to the substrate, that is to say $\Phi = \tilde{n}/t_x$. Since the number of adherent particles is much smaller than the number of particles in the chamber, it can be assumed that the concentration gradient is constant during the whole experiment, so that the particle flux is just proportional to D. The Einstein-Stokes relation gives $D \propto d^{-1}$, thus the number of particles diffusing from the inner region of the chamber and heading to the substrate per unit surface is given by

$$\tilde{n} \propto Dt_x \propto d^{-2} \qquad (10)$$

which is in agreement with the functional relationship derived in the case of pure sedimentation in (9).

Shear stress

As shown in (7), the sedimentation distance H reduces linearly with S. Therefore, it is expected a decrease in $\tilde{n}$ with S as predicted by (9) and (7). However, as long as particle sedimentation is concerned, the functional relationships $\tilde{n}$-a presented above are not affected by S.

On the other hand, if the firm particle adhesion to the substrate is concerned, the $\tilde{n}$-a relationships can be significantly affected by S. In fact, as the shear stress increases, the hydrodynamic forces acting over the particle and tending to dislodge the particle away from the substrate increase too. Even if the particle can sediment and reach the chamber floor, the shear stress can be so large to prevent the particle from firmly adhering to the substrate. With such a scenario, the size, shape and the extension of the cell-particle interface become of fundamental importance (Decuzzi and Ferrari 2006) and consequently the exponent of a in the $\tilde{n}$-a relationships can change from those derived above.

Conclusion

Size effects in the non-specific adhesion under flow of spherical particles to a confluent layer of endothelial cells is analyzed using a parallel-plate flow chamber. The number of adherent particles and their surface densities have been measured as a function of the particle diameter a, under fixed hydrodynamic conditions. Differently from prior experimental analyses, the total number of particles injected in the chamber has been changed keeping fixed the total volume of the particles. Notice that, in applications such as drug delivery and biomedical imaging, a fixed total volume of the particles corresponds to fixing the total volume of the therapeutic or imaging agents delivered to the cell layer. From the analysis of the experimental data, the following conclusions can be derived: (i) the surface density $\tilde{n}_c$ of the particles adhering to the cells decreases with the diameter a following the scaling law $d^{-1.7}$; (ii) the particles tend to adhere to the cells more avidly than to a borosilicate dish; (iii) the volume per unit surface of the particles adhering to the cells $\tilde{V}$ ($=\pi\tilde{n}_c d^3/6$) increases with the diameter a following the scaling law $d^{+1.3}$. In addition, it has been shown theoretically that a particles surface density proportional to d^{-2} is consistent with pure particles sedimentation in a linear laminar flow, in excellent agreement with the experimental results.

Observing that (i) in biomedical imaging, it is of fundamental importance to increase the number of particles adherent per unit surface ($\tilde{n}$) in order to have the largest possible spatial resolution; (ii) in the systemic delivery of drugs, it

is of fundamental importance to increase the volume $\tilde{V}_c$ of particles adherent per unit surface in order to have the largest possible amount of drug at unit surface of the target site; the two following hypothesis can be generated: (i) use the smallest possible particles in biomedical imaging and (ii) use the largest possible particles in drug delivery.

These hypotheses have been predicted and experimentally verified in the case of non-specific particle-cell interactions under small shear flow rates in in-vitro experiments. Issues related to the actual interaction of the nanoparticles within blood and with blood components, as for instance thrombogenicity, have not been considered here. However, this should not be a concern since nanoparticles to be used in-vivo are generally decorated with polymers exhibiting antithrombogenic qualities and the concentrations used are lower that the thrombogenicity concentration threshold, if one such exists for the given class of nanoparticles of interest.

Acknowledgments

We thank Dr. Camillo Palmieri at the University of Magna Graecia for valuable help in confocal microscopy.

References

Brown DC, Larson RS. 2001. Improvements to parallel plate flow chambers to reduce reagent and cellular requirements. *BMC Immunology*, 2:9.

Choi YS, Thomas T, Kotlyar A, et al. 2005. Synthesis and functional evalution of DNA-assembled polyamidoamine dendrimer clusters for cancer cell-specific targeting. *Chemistry and Biology*, (12).

Chu YS, Dufour S, Thiery JP, et al. 2005. Johnson-Kendall-Roberts theory applied to living cells. *Phys Rev Lett*, 94(2):028102.

Cohen MH, Melnik K, Boiarski AA, et al. 2003. Microfabrication of silicon-based nanoporous particulates for medical applications. *Biomedical Microdevices*, 5:253–59.

Crommelin DJA, Schreier H. 1994. Liposomes. In: Kreuter J, ed. Colloidal drug delivery systems. New York: Marcel Dekker, Inc.

Goldstein B, Zimm BH. 1971. Effect of concentration and intermolecular forces on the sedimentation of polystyrene spheres. *The Journal of Chemical Physics*, 54:4408–13.

Decuzzi P, Lee S, Bhushan B, et al. 2005. A theoretical model for the margination of particles within blood vessels. *Annals of Biomedical Engineering*, 33:179–90.

Decuzzi P, Ferrari M. 2006. The adhesive strength of non-spherical particles mediated by specific interactions *Biomaterials.* [Epub ahead of print].

Duncan R. 2003. The dawning era of polymer therapeutics. *Nat Rev Drug Discov*, 2:347–60.

Ferrari M. 2005. Nanovector therapeutics. *Curr Opin Chem Biol*, 9:343–6.

Ganong WF. 2003. Review of medical physiology, 21st ed. New York: Lange Medical Books/McGraw-Hill, Medical Publishing Division.

Goldman AJ, Cox RG, Brenner H. 1967. Slow viscous motion of a sphere parallel to a plane wall. II. Couette flow. *Chem Engn Sci*, 22:653–60.

LaVan DA, McGuire T, Langer R. 2003. Small-scale systems for in vivo drug delivery. *Nat Biotechnol*, 21:1184–91.

Matlab 6.5, Image Processing Toolbox – The MathWorks, Inc. – Copyright 1984–2002.

Rolland JP, Maynor BW, Euliss LE, et al. 2005. Direct fabrication and harvesting of monodisperse, shape specific nano-biomaterials. *J Am Chem Soc*, 127:10096–100.

van Dillen T, van Blaaderen A, Polman A. 2004. Ion beam shaping of colloidal assemblies. *Materials Today*, 40–6.

Vivek R, Patil S, Campbell CJ, et al. 2001. Particle diameter influences adhesion under flow. *Biophysical Journal*, 80:1733–43.